




Local acetate inhibits brown adipose tissue function

Wenfei Sun^{a,1,2} , Hua Dong^{a,1}, and Christian Wolfrum^{a,2}

^aInstitute of Food, Nutrition, and Health, Eidgenössische Technische Hochschule Zurich, CH 8603 Zurich, Switzerland

Edited by Christopher Glass, Department of Cellular and Molecular Medicine, University of California San Diego, La Jolla, CA; received September 16, 2021; accepted November 3, 2021

Brown adipose tissue has been extensively studied in the last decade for its potential to counteract the obesity pandemic. However, the paracrine regulation within brown tissue is largely unknown. Here, we show that local acetate directly inhibits brown fat thermogenesis, without changing acetate levels in the circulation. We demonstrate that modulating acetate within brown tissue at physiological levels blunts its function and systemically decreases energy expenditure. Using a series of transcriptomic analyses, we identified genes related to the tricarboxylic acid cycle and brown adipocyte formation, which are down-regulated upon local acetate administration. Overall, these findings demonstrate that local acetate inhibits brown fat function.

brown adipose tissue | acetate | obesity | RNA-seq

For the last 10 y, thermogenic adipose tissue is being intensively studied for its potential to combat obesity by dissipating energy in the form of heat (1–3). However, since adipose tissue harbors numerous distinct cell types, a thorough understanding of the adipose tissue microenvironment is key to harnessing the potential of thermogenic adipose tissue. Recently, we identified a subpopulation of adipocytes that release acetate, which acts as a paracrine factor regulating thermogenesis in brown adipose tissue (BAT) (4, 5). A major source of acetate is most likely the gut microbiome; however, it remains unknown to what extent gut microbiome-derived acetate can spill over into systemic circulation. Besides its conversion to acetyl-CoA, acetate can act as a signaling molecule. For example, acetate has been demonstrated to activate GPR43 in adipocytes, which results in an inhibition of lipolysis and a decrease in plasma free fatty acid levels (6, 7). Since GPR43 is expressed in a wide variety of cells, acetate may execute various roles, thereby regulating systemic metabolism. Thus, rats that received an intragastric acetate infusion for 10 d exhibited insulin resistance (8). In humans, circulating acetate was reported to be negatively correlated with insulin sensitivity (9). In accordance with previous reports (10), acetate was shown to blunt whole-body lipolysis in humans (11). Interestingly, distal, but not proximal, colonic infusion of acetate was reported to promote fat oxidation in humans (11). Of note, in the Canfora et al. study (11), fat oxidation was calculated based on O₂, CO₂, and urinary nitrogen excretion, which might be due to the fact that exogenous acetate is a substrate for fat oxidation.

Results

Based on the above-mentioned considerations, the location of acetate secretion/administration will most likely determine its physiological function (4). Therefore, it will be important to delineate the role of acetate in the context of the adipose tissue microenvironment. Here, we explored the role of acetate specifically within interscapular BAT (iBAT), by delivering acetate directly into iBAT (Fig. 1A). Acetate concentration was increased about twofold in the lobe of iBAT, which received acetate, compared to the lobe that received saline (Fig. 1B), while circulating levels of acetate remained unchanged (Fig. 1C). These levels are similar to acetate concentrations observed in iBAT under thermoneutral conditions (5). Histological analysis revealed a whitened appearance in the lobe of iBAT receiving acetate, while the other lobe retained a BAT phenotype (Fig. 1D). In accordance, UCP1 expression was significantly decreased after acetate administration (Fig. 1E). Detailed analysis

using immunohistology staining demonstrated enlarged lipid droplets and lower UCP1 expression in the acetate-receiving lobe compared to the saline lobe (Fig. 1F–J). Taken together, these data demonstrate a whitening phenotype in response to local acetate administration in a physiological range.

While we did not observe any immediate changes upon acetate delivery on energy expenditure in the initial 2 d after pump implantation (Fig. 1J), acetate administration in whole iBAT significantly reduced oxygen consumption from day 3 onward in the light phase (Fig. 1J), without any changes in movement or food consumption (Fig. 1K). To further study the physiological changes in BAT and the contribution to systemic energy expenditure, we analyzed respiration in mice in response to ADRB3 agonist (CL-316,243) administrations. Interestingly, acetate administration in iBAT could partially inhibit β -3 adrenergic activation induced oxygen consumption (Fig. 1L), suggesting that the brown fat activity is constrained by local acetate signaling. To exclude a confounding effect of the pump on tissues other than iBAT, we implanted the pump in the same anatomic location, but without a guide catheter, as illustrated in Fig. 1M. In this setting, acetate concentrations were not altered within iBAT (Fig. 1N) or serum (Fig. 1O). Thus, we can conclude that energy expenditure is not changed by catheterless acetate pump implantation, neither at basal conditions nor with β -3 adrenergic activation. Taken together, our data demonstrate that increased acetate level in iBAT inhibits brown fat activation.

In a next step, we asked whether transcriptional changes in iBAT could explain the observed phenotype. Therefore, we performed RNA sequencing (RNA-seq) of the left or right iBAT with saline, acetate, or a GPR43 agonist (CFMB) administration for 4 or 7 d, as illustrated in Fig. 2A. Unbiased hierarchical clustering, including 1,000 most variable genes expressed in at least one sample group, revealed distinct transcriptional profiles for the iBAT with local acetate or CFMB delivery (Fig. 2B). Consistent with the hierarchical clustering, a principal component analysis (PCA) showed distinct clustering of the two groups with local acetate delivery mainly in PC1 and the group with CFMB in both PC1 and PC2 (Fig. 2C). Several genes related to BAT activity—such as *Ucp1*, *Evo13*, and *Cpt1b*—were the main contributors to negative PC1 loadings (Fig. 2C). A pairwise differential gene-expression analysis, which compared the iBAT with local acetate delivery versus saline (acetate 7 d, left, versus saline 7 d, left) (Dataset S1) identified various genes related to BAT activity (Fig. 2D). Consistent with the PCA, we also found a number of genes that were down-regulated in the acetate-administrated samples versus saline to be related to BAT activity (Fig. 2E), as well as a

Author contributions: W.S., H.D., and C.W. designed research; W.S. and H.D. performed research; W.S., H.D., and C.W. analyzed data; and W.S., H.D., and C.W. wrote the paper.

The authors declare no competing interest.

This open access article is distributed under [Creative Commons Attribution-NonCommercial-NoDerivatives License 4.0 \(CC BY-NC-ND\)](https://creativecommons.org/licenses/by-nc-nd/4.0/).

¹W.S. and H.D. contributed equally to this work.

²To whom correspondence may be addressed. Email: wenfei-sun@ethz.ch or christian-wolfrum@ethz.ch.

This article contains supporting information online at <http://www.pnas.org/lookup/suppl/doi:10.1073/pnas.2116125118/-/DCSupplemental>.

Published November 29, 2021.

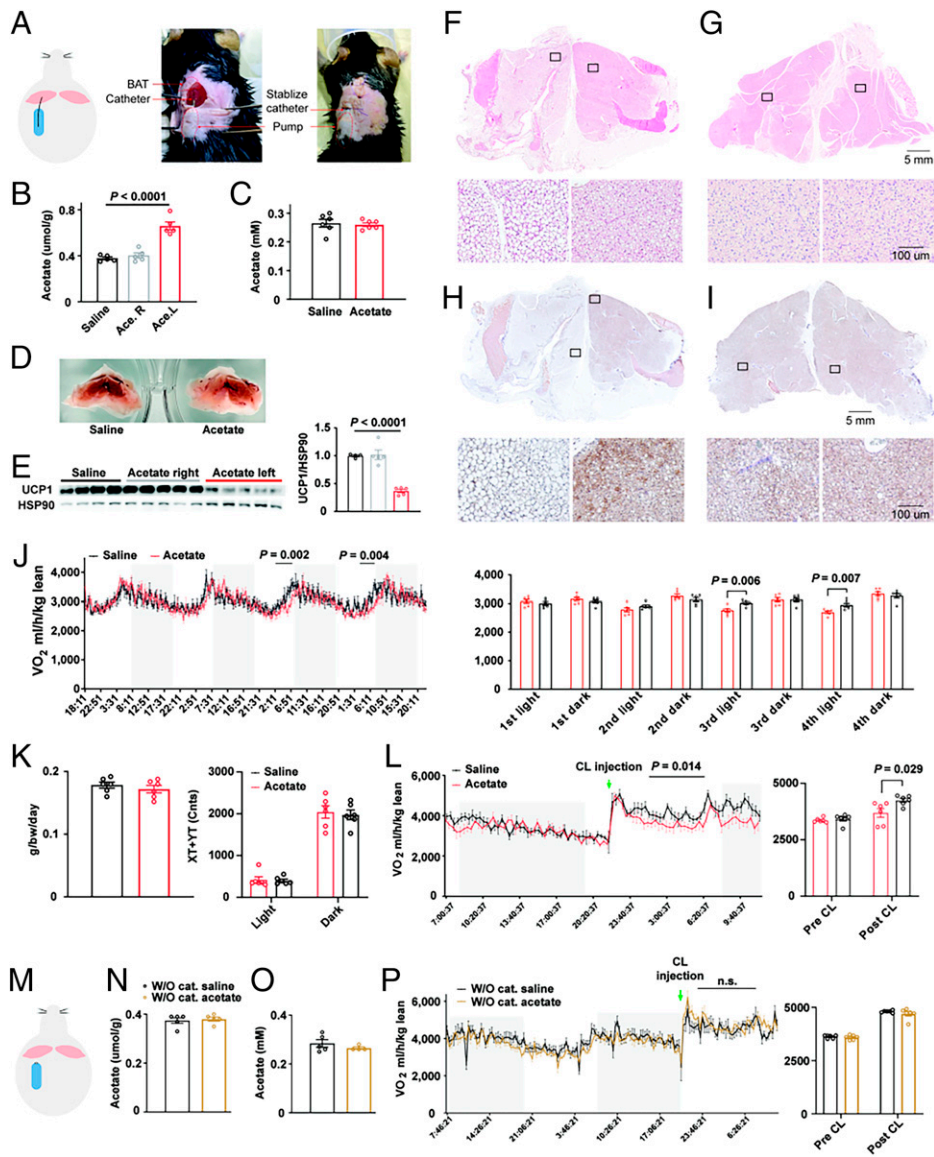


Fig. 1. (A, Left) Schematic illustration of the experimental set-up. Osmotic pumps (Alzet, 1007D) filled with sodium acetate (30 mM) or saline were implanted subcutaneously and delivered solution to left lobe of iBAT guided by a catheter, at a rate of 0.5 $\mu\text{L}/\text{h}$. (Center) The pump was implanted and catheter was connected. (Right) The catheter was stabilized by stitches. (B and C) Acetate concentration in iBAT (B, $n = 5$) and plasma (C, $n = 5$) with acetate or saline administration. (D) Representative images of iBAT with acetate and saline administration in the left lobe. (E) UCP1 protein levels in iBAT, $n = 4$ to 5. (F–I) Representative H&E (F and G) and UCP1 (H and I) staining of iBAT with acetate (F and H) and saline (G and I). (J and K) Time-resolved oxygen consumption (J), food intake and movement quantification (K) of mice with saline or acetate administration, $n = 6$. (L) Time-resolved oxygen consumption of mice upon CL injection (ADRB3 agonist CL-316,243, 0.1 mg per kg body weight, intraperitoneally), $n = 6$. (M) Schematic illustration. (N and O) Acetate level in iBAT (N) and plasma (O) of mice with pump implanted without catheter, $n = 4$ to 5. (P) Time-resolved oxygen consumption of mice upon CL injection, $n = 6$. n.s., not significant.

down-regulation of pathways related to brown adipocyte differentiation and metabolic activity (Fig. 2E). In line with RNA-seq data, *Ucp1* and *Cidea* mRNA levels were significantly lower in the iBAT lobes with either acetate or CFMB delivery (Fig. 2F).

We have previously shown that in an ex vivo brown adipocytes differentiation model, the oxygen consumption could be blocked by the addition of acetate in a dose-dependent manner (5) due to changes in brown adipocyte formation. We show here that the same inhibitory effect of acetate is observed when cells are treated at the maturation stage (Fig. 2G and H). Hence, we tested whether acetate might alter adipocyte commitment during an early developmental stage. Therefore, we differentiated stromal vascular fraction from iBAT in the presence of different amounts of acetate until day 4 of differentiation (Fig. 2I). We did not observe any differences in adipocyte formation between the different groups (Fig. 2I), and oxygen consumption was unchanged when acetate was supplemented during early adipocyte differentiation (Fig. 2K).

Discussion

In summary, our data demonstrate that local changes in acetate concentrations, at physiological levels, inhibits BAT function by

regulating brown adipocyte maturation and possibly whitening the tissue. Activation of GPR43 led to a similar response in gene expression, albeit with a reduced effect size. This could be due to the fact that acetate is a more potent regulator of GPR43 activities, possibly due to kinetics of acetate removal. Alternatively, it is possible that acetate represses the browning of iBAT by other, so far unknown pathways.

Previously it was shown that chronic intraperitoneal injection of liposome-encapsulated acetate nanoparticles could induce energy expenditure, increase voluntary movement, and enhance browning of the inguinal white adipose tissue (ingWAT) in a diet-induced obesity mouse model (12). In this context, it is worth noting that the uncoupling activity of ingWAT in diet-induced obesity models is limited, due to the low levels of *Ucp1* (13, 14), while alternate thermogenic mechanisms might be more relevant (15, 16). In the above-mentioned study, acetate was changed at a systemic level and as liposome-encapsulated nanoparticles show a distribution predominantly in liver and spleen, other organs may contribute to the observed phenotype of induced energy expenditure. Since acetate is a versatile molecule, which has been documented to have other physiological roles, such as reducing appetite via central homeostatic mechanisms (17), further studies will be needed to elucidate the autocrine versus the endocrine effects of acetate.

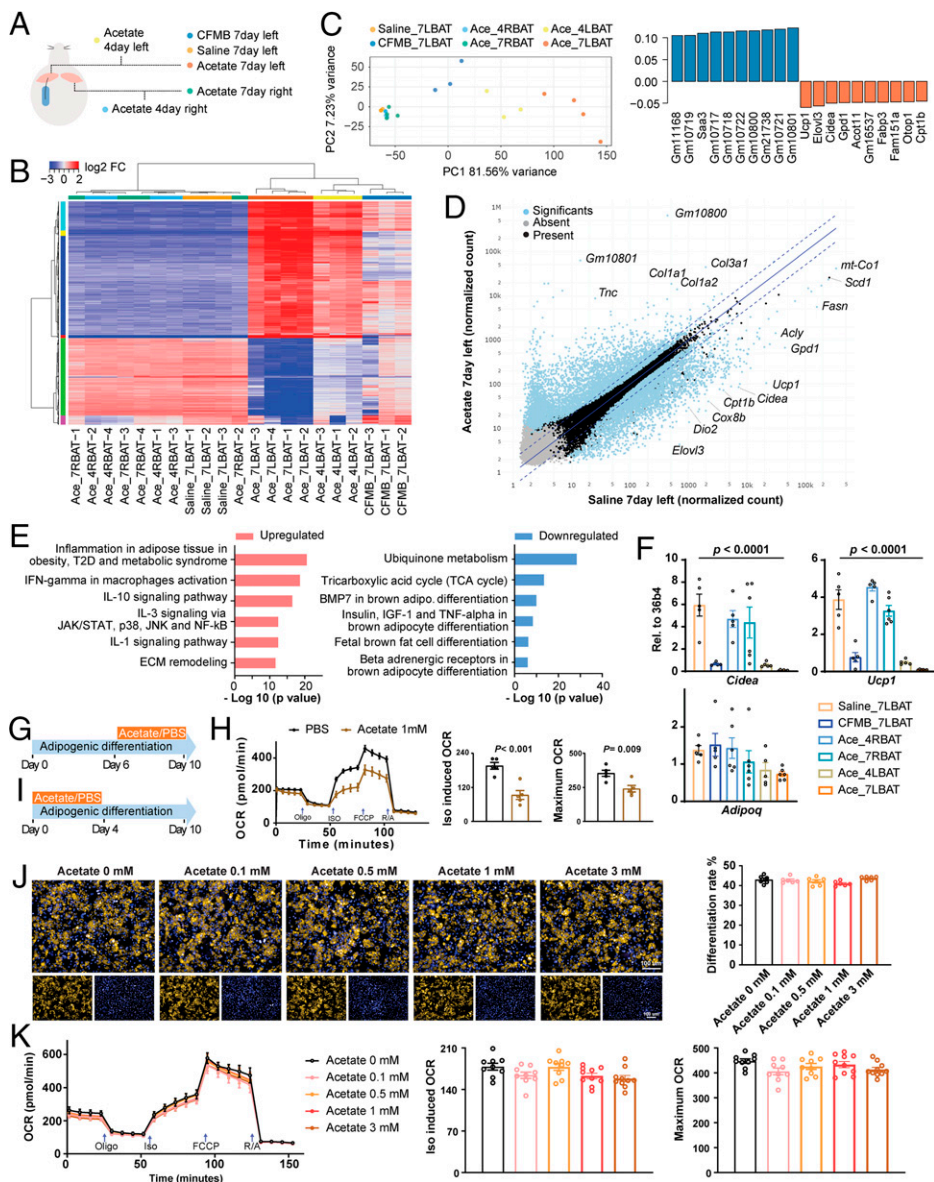


Fig. 2. (A) Schematic illustration of the samples for RNA-seq analysis. Mice were implanted with catheter-guided pump delivering saline, acetate (30 mM), or CFMB (10 μ M) to the left lobe of iBAT; the specific lobe of iBAT was collected after 4 or 7 d after implantation, as indicated. (B) Hierarchical clustering of RNA-seq data from iBAT samples is shown using a heatmap. The lengths of the branches represent the global differences between the samples, 2,000 genes with highest variance were included for the analysis, $n = 3$ to 4. (C) PCA of RNA-seq data (Left). Top 10 variable genes contributing to PC1 loading (Right). (D) Scatter plot of RNA-seq data, comparing acetate versus saline samples following 7 d of administration. Plotted are the normalized transcript counts. Significant differentially expressed genes ($P < 0.01$) are highlighted in blue, $n = 3$ to 4. (E) Metacore pathway analysis of up-regulated and down-regulated genes in iBAT samples from acetate versus saline administration, $n = 3$ to 4. (F) mRNA levels of *Adipoq*, *Ucp1*, and *Cidea* in iBAT samples analyzed by qRT-PCR, $n = 5$ to 6. (G) Schematic illustration for ex vivo adipocyte differentiation of iBAT stromal vascular fraction; acetate was supplemented from day 6 to day 10 of differentiation. (H) Time-resolved oxygen consumption rate in brown adipocytes treated with the acetate during differentiation days 6 to 10, $n = 5$. (I) Schematic illustration: acetate was supplemented from day 0 to day 4 of differentiation. (J and K) LD540 staining (*J*, $n = 6$) and time-resolved oxygen consumption rate (*K*, $n = 9$ to 10) in ex vivo differentiated cells from iBAT, treated with the indicated levels of acetate during differentiation from days 0 to 4.

Materials and Methods

All experiments were performed in adult male C57B6 mice fed ad libitum with chow diet. All animal studies were approved by the Veterinaramt Zurich. Micro-osmotic pumps (Alzet) were implanted, and libraries prepared using Truseq (Illumina). Sequencing was performed on a Novaseq-6000. Detailed procedures for pump implantation, transcriptional, and cellular analyses are described in *SI Appendix*.

1. E. D. Rosen, B. M. Spiegelman, What we talk about when we talk about fat. *Cell* **156**, 20–44 (2014).
2. B. M. Owen *et al.*, FGF21 acts centrally to induce sympathetic nerve activity, energy expenditure, and weight loss. *Cell Metab.* **20**, 670–677 (2014).
3. M. Ahmadian *et al.*, ERR γ preserves brown fat innate thermogenic activity. *Cell Rep.* **22**, 2849–2859 (2018).
4. F. Shamsi, Y.-H. Tseng, C. R. Kahn, Adipocyte microenvironment: Everybody in the neighborhood talks about the temperature. *Cell Metab.* **33**, 4–6 (2021).
5. W. Sun *et al.*, snRNA-seq reveals a subpopulation of adipocytes that regulates thermogenesis. *Nature* **587**, 98–102 (2020).
6. N. Aberdein, M. Schweizer, D. Ball, Sodium acetate decreases phosphorylation of hormone sensitive lipase in isoproterenol-stimulated 3T3-L1 mature adipocytes. *Adipocyte* **3**, 121–125 (2014).
7. Y.-H. Hong *et al.*, Acetate and propionate short chain fatty acids stimulate adipogenesis via GPCR43. *Endocrinology* **146**, 5092–5099 (2005).
8. R. J. Perry *et al.*, Acetate mediates a microbiome-brain- β -cell axis to promote metabolic syndrome. *Nature* **534**, 213–217 (2016).
9. M. Müller *et al.*, Circulating but not faecal short-chain fatty acids are related to insulin sensitivity, lipolysis and GLP-1 concentrations in humans. *Sci. Rep.* **9**, 12515 (2019).

Data Availability. RNA-seq read data have been deposited in ArrayExpress, <https://www.ebi.ac.uk/arrayexpress/> (accession no. E-MTAB-10680).

ACKNOWLEDGMENTS. We thank all other members of C.W. laboratory for suggestions and technical assistance. Transcriptomic data produced and analyzed in this paper were generated in collaboration with the Functional Genomics Center Zurich. The work was supported by Swiss National Science Foundation (SNSF) 185011 (to C.W.), SNSF 191874 (to W.S.), and SNSF 191829 (to H.D.).

10. J. R. Crouse, C. D. Gerson, L. M. DeCarli, C. S. Lieber, Role of acetate in the reduction of plasma free fatty acids produced by ethanol in man. *J. Lipid Res.* **9**, 509–512 (1968).
11. E. E. Canfora *et al.*, Colonic infusions of short-chain fatty acid mixtures promote energy metabolism in overweight/obese men: A randomized crossover trial. *Sci. Rep.* **7**, 2360 (2017).
12. M. Sahuri-Arisoylu *et al.*, Reprogramming of hepatic fat accumulation and ‘browning’ of adipose tissue by the short-chain fatty acid acetate. *Int. J. Obes.* **40**, 955–963 (2016).
13. J. Nédergaard, B. Cannon, UCP1 mRNA does not produce heat. *Biochim. Biophys. Acta* **1831**, 943–949 (2013).
14. T. D. Challa *et al.*, A genetic model to study the contribution of brown and brite adipocytes to metabolism. *Cell Rep.* **30**, 3424–3433.e4 (2020).
15. L. Kazak *et al.*, A creatine-driven substrate cycle enhances energy expenditure and thermogenesis in beige fat. *Cell* **163**, 643–655 (2015).
16. K. Ikeda *et al.*, UCP1-independent signaling involving SERCA2b-mediated calcium cycling regulates beige fat thermogenesis and systemic glucose homeostasis. *Nat. Med.* **23**, 1454–1465 (2017).
17. G. Frost *et al.*, The short-chain fatty acid acetate reduces appetite via a central homeostatic mechanism. *Nat. Commun.* **5**, 3611 (2014).